

Stability of a Chitosan Layer Deposited onto a Polyethylene Surface

Elena Pâslaru,¹ Lidija Fras Zemljic,² Matej Bračič,³ Alenka Vesel,⁴ Irena Petrinič,⁵ Cornelia Vasile¹

¹Petru Poni Institute of Macromolecular Chemistry, Physical Chemistry of Polymers Department, 41A Grigore Ghica Voda Alley, 700487 Iasi, Romania

²Faculty of Chemical Engineering, University of Maribor, Smetanova Ulica 17, SI-2000 Maribor, Slovenia

³Institute for Textile Chemistry, Faculty of Mechanical Engineering, Laboratory for Characterization and Processing of Polymers, University of Maribor, Smetanova Ulica 17, SI-2000 Maribor, Slovenia

⁴Jožef Stefan Institute, Jamova 39, 1000 Ljubljana, Slovenia

⁵Center of Excellence for Polymer Materials and Technologies, Tehnološki Park 24, 1000 Ljubljana, Slovenia

Correspondence to: C. Vasile (E-mail: cvasile@icmpp.ro)

ABSTRACT: A two-step procedure was applied to obtain antimicrobial films; this procedure involved a corona treatment of the polyethylene (PE) surface and its chemical activation with 1-ethyl-3-[3-dimethylaminopropyl] carbodiimide hydrochloride and *N*-hydroxysuccinimide, and this led to the covalent bonding of chitosan on the PE surface. Electrochemical methods were used to investigate the stability of the deposited chitosan layer. The potentiometric and polyelectrolyte titrations showed that some amount of chitosan desorbed faster from the surface until equilibrium was reached and also that the grafted chitosan layer was more stable than the physically adsorbed one. The chitosan immobilized on the PE surface exhibited the expected antibacterial activity when tested against three bacteria, which included two Gram-negative bacteria, *Salmonella enteritidis* and *Escherichia coli*, and one Gram-positive bacterium, *Listeria monocytogenes*.

© 2013 Wiley Periodicals, Inc. *J. Appl. Polym. Sci.* 130: 2444–2457, 2013

KEYWORDS: functionalization of polymers; packaging; polyolefins; polysaccharides

Received 8 January 2013; accepted 19 March 2013; Published online 27 May 2013

DOI: 10.1002/app.39329

INTRODUCTION

Despite the considerable research and development efforts made through the years, the problem of infections related to biomedical devices and implants persists. Bacteria evidently can readily colonize the surfaces of synthetic materials, such as those used for the fabrication of catheters, hip and knee implants, and many other devices. There is a strong need to mitigate bacterial colonization by the modification of the surfaces of biomedical devices and implants and impart to them features such as surface chemistry and surface roughness to prevent bacterial attachment.¹

Bacterial adhesion onto surfaces is the first event in a series of host and organism reactions. Adhesion is mediated by physicochemical interactions between the bacteria and the biomaterial's surface. Hence, the surface modification of biomaterials or devices is a relatively straightforward strategy for creating desirable surfaces that will decrease the surface susceptibility to bacterial adhesion.²

Most medical devices, such as prostheses, bone replacement implants, drug-delivery devices, tissue engineering devices, and catheters, are made of synthetic polymers. These polymers are easily processable into desirable shapes at low costs, yet they

lack biocompatibility and biodegradability. Despite the considerable success achieved with the use of synthetic polymers in medical devices and food packaging, their surfaces are susceptible to bacterial colonization; this creates important public health concerns. Surface modification is one of the solutions recommended to prevent infections and to prolong the shelf life of these devices and the safety of food products.³

Low-density polyethylene (LDPE) is a heat-sealable, inert, odor-free material that shrinks when heated. It acts as a good moisture barrier but it has a relatively high gas permeability, high sensitivity to oils, and poor odor resistance. It is less expensive than most films and is, therefore, widely used.⁴

Chitosan is a biopolymer with a good antimicrobial ability because it inhibits the growth of a wide variety of fungi, yeasts, and bacteria.^{5,6} In addition, it forms a clear, tough, flexible film almost by itself after its dissolution in an acidic solution and acts as a good oxygen barrier.^{7,8}

Several studies have been devoted to the improvement in the quality (especially the antimicrobial properties) of LDPE food packaging films by chitosan. Both Gram-positive and Gram-negative

bacteria were inhibited by antimicrobial LDPE films containing more than 1.43 wt % of incorporated chitosan.^{9,10}

For inert polymers, such as polyethylene (PE), the polymer backbone requires functionalization before the bioactive agent of interest can be attached or generated. The simplest methods for laboratory use involve wet chemical oxidations of the polymer surface with, for example, chromium trioxide, potassium hypochlorite, or potassium permanganate in concentrated sulfuric acid.^{11,12} In a study developed by Lin et al.,¹³ chitosan was used to modify the inner surface of an oxidized PE tubing device used for biliary stent applications by a methanol precipitation technique. The commercial application of wet chemical modifications is limited by numerous safety and environmental concerns because of the toxicity of the chemicals used. Plasma treatment technologies are likely to be the most useful commercial techniques for the controlled surface functionalization of a broad range of polymers.¹⁴ Corona-discharge oxidizes the film surface, introducing a series of oxygen and nitrogen-containing functional groups onto the polymer backbone.¹⁵ Shin et al.¹⁶ applied the plasma source ion implantation technique to the improvement of the adhesion between linear LDPE and chitosan or corn zein.

A recent publication by Theapsak et al.¹⁷ presents the preparation of a chitosan-coated PE film by dielectric barrier discharge (DBD) under medium vacuum pressure in the presence of air gas. The authors claimed that the functional groups implanted onto the PE surface after DBD treatment enabled the formation of ester linkages between the PE surface and chitosan and also that the obtained surface exhibited antibacterial activity against *Escherichia coli* and *Staphylococcus aureus*.

Following the previous studies and taking into account the low number of carboxyl groups that could be implanted onto the PE surface by DBD treatment, we concluded that a simple corona or DBD treatment of PE was not sufficient to provide a stable chitosan layer over time. This study dealt with functionalization of PE by chitosan, with a two-step procedure involving corona treatment at atmospheric pressure followed by carbodiimide coupling chemistry; this enabled stronger covalent linking between the PE surface and chitosan and thus assured the stability of the coating. To determine the efficiency of the coating methodology and the influence of the two-step procedure on the quality of surface coating, the PE surfaces were analyzed by different methods. The stability of the deposited chitosan layer in media of different pH (at both neutral and acidic pH) was investigated. The corona-discharge-treated polyethylene (PE_{cor}) films subsequently coated/grafted with chitosan were physicochemically analyzed by attenuated total reflection (ATR)–Fourier transform infrared (FTIR) spectroscopy, X-ray photoelectron spectroscopy (XPS), potentiometric titration, ζ -potential (ZP) measurements, and polyelectrolyte titration, and the antimicrobial activity was tested against some pathogenic microorganisms, including Gram-positive (*Listeria monocytogenes*) and Gram-negative (*E. coli* and *Salmonella enteritidis*) bacteria.

EXPERIMENTAL

Materials

PE, 0.02 mm thick and purchased from SC LORACOM SRL (Roman, Romania), was used. The PE was composed of two parts

UV-treated LDPE (Tipolen, Tiszai Vegyi, Hungary) and one part high-density polyethylene (HDPE; SIDPEC, Egypt), respectively.

Low-molecular chitosan (CHT), with a 20–300-cP dynamic viscosity in 1% acetic acid and a 75–85% deacetylation degree, was purchased from Sigma-Aldrich (Steinheim, Germany).

Ethanol (96%) and glacial acetic acid (99.5%) were purchased from Chemical Co. (Iasi, Romania). A water-soluble carbodiimide crosslinker for the zero-length carboxyl-to-amine conjugation of 1-ethyl-3-[3-dimethylaminopropyl] carbodiimide hydrochloride (EDC) and *N*-hydroxysuccinimide (NHS; Thermo Scientific Pierce Protein Research Products) were used. The excess reagent and the crosslinking byproducts were easily removed by washing with water or dilute acid.

Corona Treatment of the PE Films

The corona treatment of PE was performed before chitosan deposition with atmospheric plasma by means of an Enerkon Corona Osman Onder instrument.

The PE film was placed between two electrodes subjected to a difference of potential. The treatment station applied a 50/60 Hz electrical power to the surface of the material through an air gap via a pair of electrodes at high potential and a roll at ground potential, which supported the material. Only the side of the material facing the high-voltage electrode should have shown an increase in surface tension. Atmospheric air was chosen as the gas, and the following parameters were used: a frequency of 30 kHz, an interelectrode distance of 7 mm, and a plasma treatment power of about 45 kJ/m².

After the corona-discharge pretreatment, the PE surface was enriched with oxygen-containing groups, such as carboxyl, carbonyl, hydroxyl, and/or ester groups.

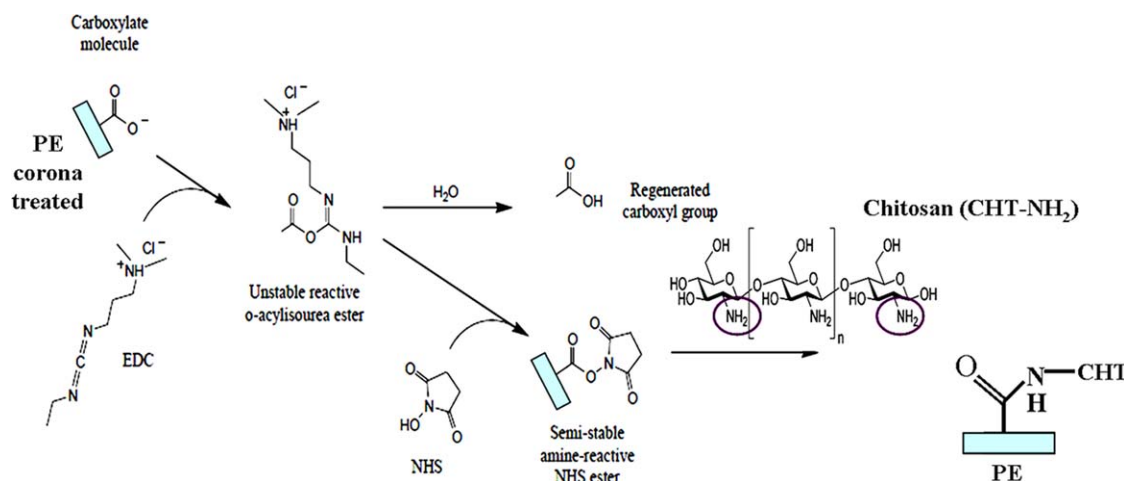
Functionalization of the PE Surface: Coating/Immobilization Procedures

Chitosan coating on the PE surface was achieved by the dipping of the PE_{cor} films into chitosan solutions with 1 wt % concentration. This concentration value was selected after a study of the influence of this parameter, which gave similar results to those presented by Theapsak et al.¹⁷

The chitosan solutions were prepared in twice-distilled water containing 8% acetic acid and 30% ethanol to facilitate film formation and solvent evaporation.

Covalent Bonding. Chitosan was immobilized (covalently attached) on the PE_{cor} film surface by means of coupling agents (EDC and NHS). EDC is a zero-length crosslinking agent used to couple carboxyl groups to primary amines. EDC reacts with a carboxyl to form an amine-reactive *O*-acylisourea intermediate. If this intermediate does not encounter an amine, it will hydrolyze and regenerate the carboxyl groups. In the presence of NHS, EDC can be used to convert the carboxyl groups to amine-reactive NHS esters. This is accomplished by the mixing of EDC with a carboxyl-containing molecule and is followed by NHS addition. Through the combination of EDC and NHS, amine-reactive NHS esters can be created as intermediates on any carboxyl-containing molecule.

An aqueous solution of 75 mM EDC and 15 mM NHS was used to activate the carboxylic groups formed at the PE surface



Scheme 1. Possible reaction scheme between the corona-activated PE surface and chitosan with crosslinking agents (adapted from refs. 18–20). [Color figure can be viewed in the online issue, which is available at wileyonlinelibrary.com.]

after corona pretreatment. When the activated PE film was immersed in the chitosan solution, the activated carboxylic groups formed at the surface after corona-discharge exposure reacted with the chitosan amino groups to form stable amide bonds, according to Scheme 1.

Other reactions were also possible because of the high reactivity of the active species created by plasma exposure and the functional groups of chitosan.

The chitosan-coated films were washed with double-distilled water and dried, first at room temperature and subsequently *in vacuo*, at 50°C for 24 h. The thus prepared samples were analyzed by various methods.

The coated and grafted untreated PE films and PE_{cor} films were investigated comparatively with the untreated PE film, which was used as a reference (Table I). Desorption studies were performed at various pHs (the sample notation indicates the pH value involved; see Table I).

Investigation Methods

Chitosan Coating of the PE Surface. ATR–FTIR spectroscopy.

The ATR–FTIR spectra were recorded on a Bruker VERTEX 70 spectrometer in transmittance mode with a 4-cm⁻¹ resolution. The background and sample spectra were obtained in the 600–4000 cm⁻¹ wave-number range. Spectral processing was achieved with the SPECVIEW program.

XPS. XPS analysis was carried out with a thin film analysis XPS Physical Electronics instrument. The basic pressure in the chamber was about 6×10^{-8} Pa. The samples were excited with X-rays over a 400- μ m spot area with monochromatic Al K $\alpha_{1,2}$ radiation at 1486.6 eV. The photoelectrons were detected with a hemispherical analyzer positioned at an angle of 45° with respect to the normal of the sample surface. Survey-scan spectra were recorded at a pass energy of 187.85 eV and with a 0.4-eV energy step, whereas high-resolution spectra of the C1s carbon were obtained at a pass energy of 23.5 eV and with a 0.1-eV energy step. An electron gun was used for surface neutralization.

The concentration of elements was determined with MultiPak v7.3.1 software from Physical Electronics, supplied together with the spectrometer. XPS survey spectra were taken at least at two different spots on the surface, and the results obtained are given as an average.

Potentiometric titration. Potentiometric titration was used for the direct determination of the amino groups on the PE surface. The theoretical principle behind potentiometric determinations was well described by Fras et al.²¹ A two-burette instrument (Mettler-Toledo) equipped with a combined glass electrode (Mettler T DG 117) was used. The burettes were filled with 0.1M HCl (Fluka, analytical) and 0.1M KOH (Baker, diluted). All solutions were prepared with deionized water with a very low carbonate content, which was obtained by boiling and subsequent cooling under a nitrogen atmosphere.

The PE films coated with chitosan and the reference PE were titrated in forward and back runs at pH values ranging between 2.8 and 11. The titration experiments were carried out at a 0.1M ionic strength, set to its appropriate value with KCl (Riedel-de-Häen, Germany). The titrant was added at varied preset intervals of 0.001–0.25 mL. The stability criterion for taking a reading after each addition was set to $dE/dt = 0.1$ mV/30 s, where E is the first derivative of the potential in respect with time (t), 30 s was the minimum time needed to reach equilibrium conditions between the two additions of the titrant, and the maximum time was set to 180 s. Further on, the blank HCl–KOH titration was carried out under the same conditions.

The titration of the chitosan solution with an excess amount of HCl was expected to be similar to that of the mixture of a strong acid (excess HCl) and a weak acid ($-\text{NH}_3^+$ of chitosan). In this case, it is generally approximated that the amount of weak acid titrated is equal to the amount of base consumed between the first and second inflection points of the titration curve. The pK_a value of the $-\text{NH}_3^+$ group can be estimated from the midpoint of the titration curve. At this point, half of the amino groups are in protonated state and half of them are in deprotonated state.

Table I. Notations and Descriptions of the Investigated Samples

Sample notation	Sample description
PE	Untreated PE film
CHT	Chitosan
PE/CHT	Untreated, chitosan-coated PE film
PE _{cor} /CHT	Corona-treated, chitosan-coated PE film
PE/EDC + NHS/CHT	Untreated PE film immersed in an aqueous solution of the coupling agents EDC and NHS and further coated with chitosan
PE _{cor} /EDC + NHS/CHT	Corona-treated PE film activated with EDC + NHS and coated with CHT
PE/CHT, pH 3.6 (6.5)	Corona-untreated PE film coated with CHT and with desorption at pH 3.6 or 6.5
PE _{cor} , pH 3.6 (6.5)	Corona-treated PE film coated with CHT and with desorption at pH 3.6 or 6.5
PE/EDC + NHS/CHT, pH 3.6 (6.5)	Corona-untreated PE film activated with an EDC + NHS solution, coated with CHT, and with desorption at pH 3.6 or 6.5
PE _{cor} /EDC + NHS/CHT, pH 3.6 (6.5)	Corona-treated PE film activated with an EDC + NHS solution, coated with CHT, and with desorption at pH 3.6 or 6.5

With the Henderson–Hasselbalch eq. (1) (with consideration of the ionization of the weak acid HA), we calculated the pK_a :

$$pH = pK_a + \log \left(\frac{[A^-]}{[HA]} \right) \quad (1)$$

where $pK_a = -\log K_a$ (where K_a is the dissociation constant), $[HA]$ represents the molar concentration of a weak acid, and $[A^-]$ is the molar concentration of the dissociated ion.

In this particular case of chitosan, the Henderson–Hasselbalch equation becomes eq. (2):²²

$$pH = pK_a + \log \left(\frac{[NH_2]}{[NH_3^+]} \right) \quad (2)$$

where pH is the solution pH, pK_a is the acid dissociation constant, $[NH_2]$ is the concentration of the amine groups, and $[NH_3^+]$ is concentration of the protonated amine groups.

ZP measurements. ZP was determined with a SurPASS electrokinetic analyzer on the basis of the streaming current and streaming potential measurement methods used for flat solid surfaces.^{23–27} The latter enables the calculation of a correct ZP without approximation. The ZP of flat surfaces can be determined with two different rectangular measuring cells: the clamping cell and the adjustable gap cell. In our case, the adjustable gap cell was used for ZP measurements.

Evaluation of the Chitosan Desorption. Polyelectrolyte titration. An amount of 0.05 g of sample was immersed for 48 h in 50 mL of aqueous solution at different pH values (3.6 and 6.5, adjusted by 0.1M hydrochloric acid). The solution was filtered at pre-established times, and the filtrates were further used for polyelectrolyte titration. The analyte was composed of 38 mL of distilled water, 1 mL of *ortho*-toluidine blue indicator (Sigma-Aldrich), and 1 mL of the filtered solution (desorbed chitosan). A Mettler-Toledo DL 53 titrator with a 10-mL burette was used for the incremental addition of the polyelectrolyte titrant [polyethylenesulfonate sodium salt (PES-Na); concentration = 10 mM]. Incremental additions of 100 μ L were performed every 3–10 s. The absorbance was measured as a potential change in

millivolts with a Mettler-Toledo Phototrode DP660 at a wavelength of 660 nm. $[NH_3^+]$ was determined from the equivalent volume (V) of the added PES-Na solution, which was detected as the steep step in the absorbance versus V (PES-Na) titration curve and by the estimation of a 1:1 binding stoichiometry of ethylenesulfonate to the chitosan amine groups.

After the chitosan-desorption experiments, the PE surfaces were dried at 50°C and investigated by ATR–FTIR spectroscopy and potentiometric titration under the previously described conditions.

Antimicrobial tests. Antimicrobial tests were performed by well-known standard methods such as the following:

- SR ISO 16649-2/2007: Microbiology of food and animal feeding stuffs: This is a horizontal method for the enumeration of β -glucuronidase-positive *E. coli*. It included a colony-counting technique at 44°C with 5-bromo-4-chloro-3-indolyl β -D-glucuronide. The most probable number of β -glucuronidase-positive *E. coli* was determined according to the number of tubes of Minerals Modified Glutamate Broth (catalog number 1365), whose subcultures produced blue or blue-green colonies on tryptone bile glucuronide agar. This was inoculated and incubated at a temperature of 44°C for 20–48 h.
- SR EN ISO 11290-1:2000/A1:2005, part 1: Detection method, amendment 1: Microbiology of food and animal feeding stuffs: This is a horizontal method for the detection and enumeration of *L. monocytogenes*.
- SR EN ISO 6579/2003/AC/2004/AC/2006, amendment 1:2007: This is a horizontal method for the detection of *Salmonella spp.* bacteria, approved by European Committee for Standardization as EN ISO 6579:2002.

RESULTS AND DISCUSSION

Chitosan Coating of the PE Surface

ATR–FTIR Results. The ATR–FTIR spectra for the PE surfaces coated with chitosan are shown in Figure 1.

The FTIR spectrum of chitosan (Figure 1, spectrum 7) showed a broad —OH stretching absorption band between 3550 and 3030

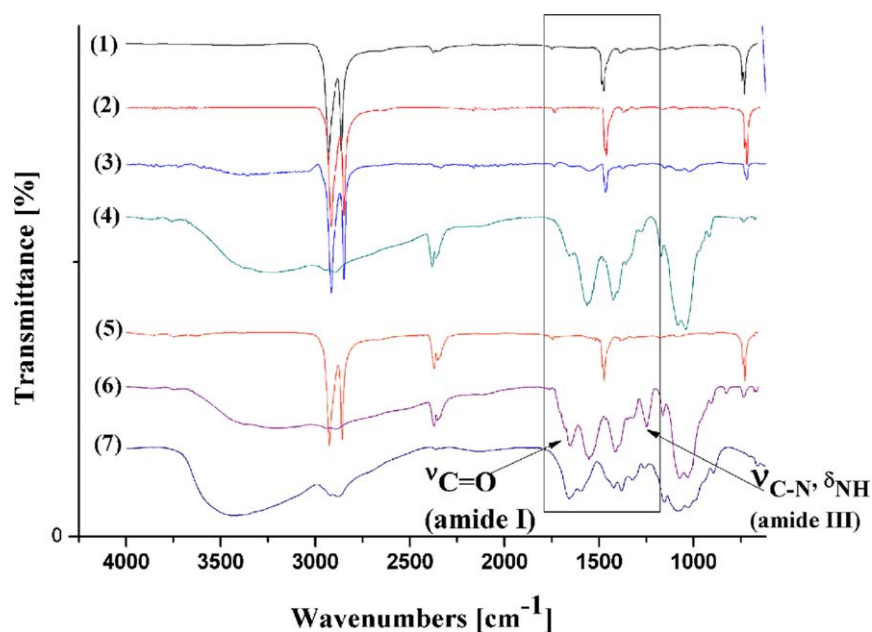


Figure 1. ATR-FTIR spectral comparison of PE films coated with chitosan by different methods, namely, physical adsorption and grafting: (1) PE, (2) PE_{cor}, (3) PE/CHT, (4) PE_{cor}/CHT, (5) PE/EDC + NHS/CHT, (6) PE_{cor}/EDC + NHS/CHT, and (7) CHT. [Color figure can be viewed in the online issue, which is available at wileyonlinelibrary.com.]

cm^{-1} and aliphatic C—H stretching between 2980 and 2830 cm^{-1} .²⁸ When the —OH and the aliphatic C—H stretching bands were aligned, they appeared in the spectrum as a broad band from 3550 to 2830 cm^{-1} . Another major absorption band with a maximum at 1597 cm^{-1} represented the free primary amino groups (—NH₂ bending) at the C₂ position of glucosamine, a major group present in chitosan. The peak at 1657 cm^{-1} represented the acetylated amino groups in chitin and indicated that the sample was not fully deacetylated (the chitosan used had a 75–85% deacetylation degree). The peak at 1384 cm^{-1} represented the —C—O stretching of the primary alcoholic group (—CH₂—OH). The absorption bands at 1155 cm^{-1} (antisymmetrical stretching of the C—O—C bridge) and 1081 and 1029 cm^{-1} (skeletal vibration involving C—O stretching overlapped with the —NH₂ stretching vibration) were characteristic of the saccharide structure of chitosan.

Spectrum 3 (Figure 1) showed that the chitosan absorption bands with small intensities (the —OH stretching and aliphatic C—H stretching bands at 3550–2830 cm^{-1} and the —NH₂ band at 1597 cm^{-1}) appeared when PE was not pretreated with corona discharge. In this case, some viscous chitosan solution stuck only physically to the surface after drying, although after corona treatment, the characteristic IR bands of chitosan (Figure 1, spectrum 4) were much more intense and well-defined, with the chitosan coating being significant only after corona treatment. Furthermore, mention should be made of the fact that after corona pretreatment, the coating was more uniform, and the chitosan layer was thicker than that of the untreated corona surface (see Figure 2). This assertion was proven by the presence in the IR spectrum of untreated corona PE and the chitosan-coated sample of the PE characteristic vibration bands (CH stretching at 2916–2847 cm^{-1}), even when an overlapping

vibration band occurred in this spectral region. For example, the IR spectrum of the PE/CHT sample (Figure 1, spectrum 3) revealed chitosan's characteristic bands with a flattened aspect, whereas two sharp and narrow bands assigned to PE were present in the 2916–2847- cm^{-1} range. On the contrary, in this last region, for a corona-treated sample (Figure 1, spectrum 4), this shoulder became broader, was no longer divided into two parts, and was assigned only to chitosan. The bands characteristic of PE no longer appeared in the IR spectra; this indicated a good chitosan-coated surface. Similar spectral modifications were also found in the ATR-FTIR spectra of the corona-treated samples activated with the coupling agents EDC + NHS (Figure 1, spectrum 6). Moreover, three particular bands localized at 1654, 1547, and 1258 cm^{-1} and assigned to the stretching vibrations of —C=O (amide I), amide N—H bending, and C—N stretching vibrations (amide II), respectively, and a complex band consisting of C—N stretching and N—H in-plane deformation vibrations (amide III band), respectively, were used to assess the covalent bonding of chitosan on the PE surface.^{29,30}

Theoretically, in the case of grafted samples, the amount of desorbed chitosan from the PE surface should be lower, as demonstrated by subsequent gravimetric and desorption studies.

Chitosan Layer Thickness. The initial thickness of the PE films was 0.02 mm. The average mass and thickness of the chitosan layer deposited on the PE surface was determined by high-precision weighing (gravimetric method) and automatic micrometer measurements, respectively. The results are listed in Table II.

We easily observed that the mass and thickness of the chitosan layer were higher after corona-discharge exposure of the substrate.

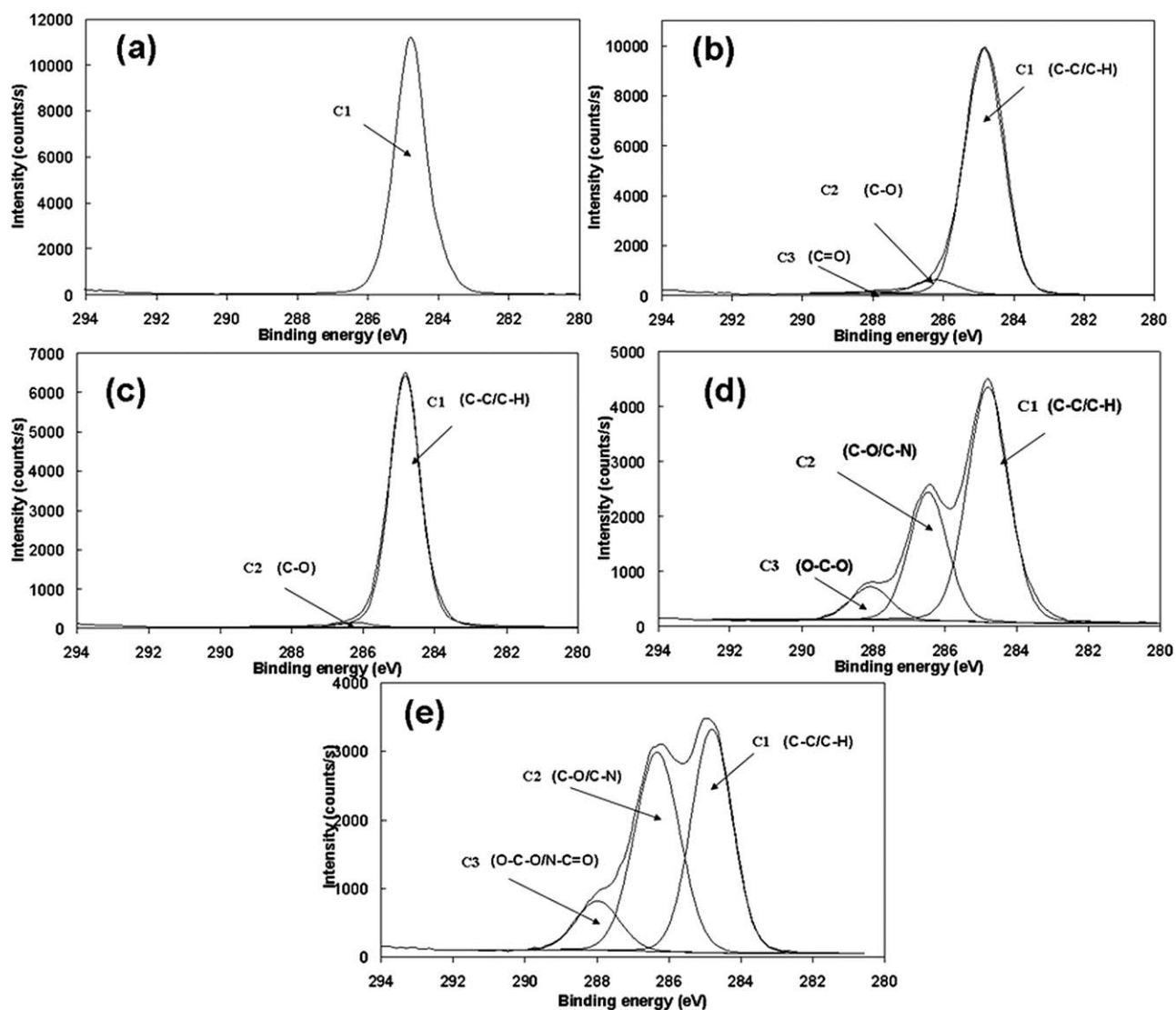


Figure 2. High-resolution carbon peaks of (a) PE (reference), (b) PE_{cor}, (c) PE/CHT, (d) PE_{cor}/CHT, and (e) PE_{cor}/EDC + NHS/CHT.

Surface Chemical Composition Determined by XPS. The surface chemical composition and atomic concentrations (%) of the pristine PE film, PE_{cor} film, and chitosan-coated film were obtained with XPS survey-scan spectra (Table III) measured at two different spots on the surface of each sample.

A useful comparison of the survey spectra revealed that carbon was the predominant species (usually found on the neat PE

surface); traces of oxygen, resulting from partial oxidation, and traces of impurities were also found. After the corona treatment of the PE surface, the carbon content decreased from 99.2 to 94.2%, and the oxygen amount increased up to 5.6%; this indicated implementation of the oxygen-containing functionalities, which improved the adhesion of the chitosan on the PE surface and confirmed the covalent bonding via the previously described coupling reaction. The C content of the PE surface was reduced after the corona-discharge treatment, probably because of chain breaking at the polymer surface and chemical reorganization induced by the electrons generated during corona discharge. Coating with chitosan led further to important changes in the surface composition of the samples. In the case of the untreated film, no N component was detected on the sample surface, and this was consistent with the absence of nitrogen in the PE structure. As expected, new O and N emission peaks appeared in the XPS spectra of the modified PE samples because of subsequent chitosan coating. The oxygen content increased up to 25 atom %, whereas the nitrogen

Table II. Mass and Thickness of the Deposited CHT onto the PE Surface

Sample	CHT mass (mg/cm ²)	Thickness of the CHT layer (μm)
PE/CHT	25.2	5
PE _{cor} /CHT	285.2	30
PE/EDC + NHS/CHT	23.1	4
PE _{cor} /EDC + NHS/CHT	263.2	25

Table III. Experimental Atomic Composition (atom %) Obtained from the XPS Survey Spectra for the Corona-Treated and Chitosan-Modified PE

Sample	C (atom %)	O (atom %)	N (atom %)
PE	99.2 ± 0.3	0.8 ± 0.1	—
PE _{cor}	94.2 ± 0.3	5.6 ± 0.1	—
PE/CHT	92.0 ± 1.6	6.7 ± 1.0	—
PE _{cor} /CHT	70.2 ± 0.5	23.1 ± 0.6	4.4 ± 0.1
PE _{cor} /EDC + NHS/CHT	69.8 ± 0.3	24.9 ± 0.3	5.4 ± 0.02

amount even reached 5.4 atom %. The most significant change in the surface composition was observed for the PE_{cor}/EDC + NHS/CHT sample.

Because the only source of nitrogen on the PE surface was represented by the chitosan coating, the atomic content of nitrogen could be used for the evaluation of coating efficiency. The highest atomic percentage of nitrogen was found for the PE_{cor}/EDC + NHS/CHT sample; therefore, the grafting procedure could be considered to be the most efficient.

Figure 2 provides the high-resolution C1s–XPS spectra for both the untreated and the modified PE samples, with the variation of the corresponding areas evidencing the differences between the samples (Table IV). The C1s spectrum of PE [Figure 2(a)] showed a single peak at 284.8 eV, whereas the C1s spectra of the other samples could be curve-fitted with two or three peak components, from chemically nonequivalent carbon atoms mainly bonded to oxygen for the corona-treated samples to nitrogen for the chitosan-coated ones.

According to literature data, for the PE C1s spectrum [Figure 2(a)], the peak at 284.8 eV (denoted as C1) could be assigned to the C–C and C–H bonds. In the case of the PE_{cor} sample, the deconvoluted C1s core-level spectrum consisted of three peaks [C1, C2, and C3; Figure 2(b)]. The first, situated at 284.9 eV, could be assigned to C–C/C–H bonding. The second peak, located at 286.2 eV, was attributed to the chemical bonding of C in the C–O bond, and the third one, located at 287.9 eV, was related to C=O bonding.^{31–34}

The C1s spectra of the PE_{cor}/CHT and PE_{cor}/EDC + NHS/CHT samples could be curve-fitted with three peak components. From chemically nonequivalent carbon atoms, two major peaks (denoted as C1 and C2) at 284.8 and 286.4 eV were related to C–C and C–N species, respectively, and one smaller peak

(denoted as C3) at 288.0 eV was attributed to the C in the amide bonds N–C=O and/or O–C–O chemical bonding in the chitosan's sugar residues. Covalent bonding did not change the position of the last mentioned peak and only caused variation of the peak area.

Chitosan grafting onto the PE_{cor} surface was achieved by the formation of amide bonds between the surfaces containing oxygen functionalities and chitosan's amino groups by means of coupling agents (i.e., EDC + NHS). As to the concentration of various bonds on the surface (Table IV), we observed that the use of the EDC + NHS coupling agents led to an increase in the C3 peak area, which was directly proportional to its atomic concentration. This signal may have been due to the C from N–C=O bonding, a fact that proved that the exploitation of the coupling agents was more favorable for chitosan immobilization onto the PE surface, with the amide bond being a chemically stable one. This assertion was also supported by the ATR–FTIR results, as according to the previous data, new amide bonds were evidenced. Not all of the amino groups of chitosan were involved in the coupling reaction, and free amino groups were still present on the surface, ensuring antimicrobial activity, as is demonstrated in the following section.

Amino Group Determination by Potentiometric Titration.

The potentiometric titration curves for the reference PE, chitosan, and chitosan-coated PE films are shown in Figure 3.

With eq. (2) (see Experimental section), the p*K*_a values were calculated for all of the investigated samples. In the case of chitosan, we found a p*K*_a value equal to 6.5. For the chitosan-coated PE samples, the calculated p*K*_a values were as follows: for PE_{cor}/EDC + NHS/CHT, the p*K*_a was 5.9, and for PE_{cor}/CHT, it was found to be 5.7. In both cases, the experimentally obtained p*K*_a value was close to that of native chitosan; this proved the efficiency of the coating process.

As is well known, chitosan possesses ionizable groups in its structure, namely, primary amino groups. In our case, the main source for the positive charge was protonation of the chitosan amino groups when the pH was changing. The surface charge amount was calculated from the plateau level of the charging isotherms (Figure 3). Figure 4 shows the surface charge amount for the PE and chitosan-coated PE.

We noted that the positive charge increased after corona-discharge treatment and chitosan coating. In the PE_{cor}/CHT sample, we found a total charge amount value (113.04 mmol/kg) that was slightly higher than that for the PE_{cor}/EDC + NHS/CHT sample (94.78 mmol/kg). In the latter case, the variation

Table IV. Binding Energies (eV) of the Carbon Atoms and Area (atom %) of the C1s Peaks for the Untreated and Chitosan-Coated PE Samples

Sample	PE			PE _{cor}			PE/CHT			PE _{cor} /CHT			PE _{cor} /EDC + NHS/CHT		
	C1	C2	C3	C1	C2	C3	C1	C2	C3	C1	C2	C3	C1	C2	C3
Binding energy (eV)	284.8	—	—	284.9	286.2	287.9	284.8	286.2	—	284.8	286.5	288.1	284.9	286.4	288.0
Area (atom %)	100	—	—	94.3	4.9	0.8	98.1	1.9	—	60.7	31.0	8.3	45.2	44.2	10.6

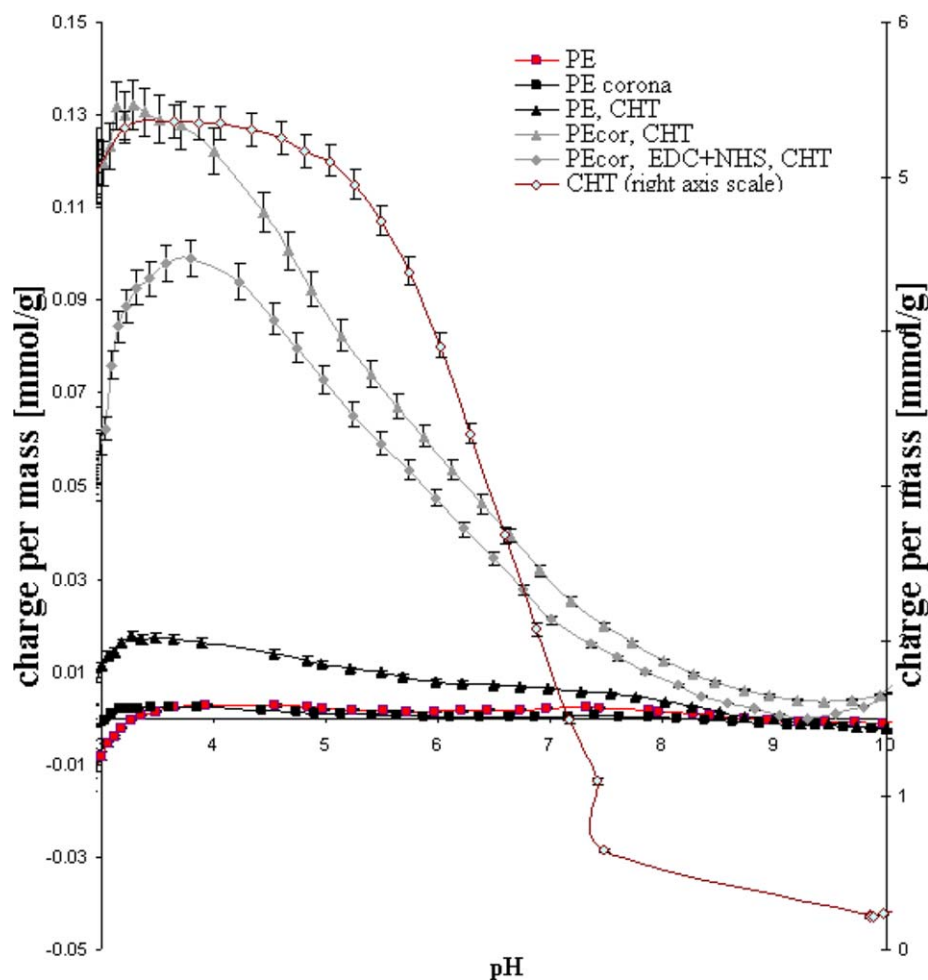


Figure 3. Potentiometric titration curves for the PE and chitosan-based samples: PE, PE_{cor}, PE/CHT, PE_{cor}/CHT, PE_{cor}/EDC + NHS/CHT, and CHT. [Color figure can be viewed in the online issue, which is available at wileyonlinelibrary.com.]

may have been due to a decrease in the number of amino groups that could be protonated; this was caused by the coupling reaction and the formation of amide bonds.

ZP Evaluation. The ZP or the electrokinetic potential originates from the accumulation of electrical charges at a solid/liquid interface. As an indicator for surface charge, the ZP gives information about adsorption or adhesion processes and also about the existence of acidic and basic surface groups.

The shape of the curve for untreated PE was typical for polymers bearing no dissociating groups; however, it exhibited an isoelectric point (IEP) around pH 2.5, which was close to the values given in the literature^{35,36} (Figure 6, shown later). Beneš and Paulenová³⁵ found out that the H⁺ and OH⁻ ions are potential-determining on the PE surface. Because of the hydrophobic characteristics of the unmodified PE, the preferential adsorption of the chloride anions, which gave a negative ZP in the pH range of 3–9 range was observed. The negatively charged surface of PE was probably due to the dissociation of some polar groups (e.g., carboxyl groups) contained on the PE surface as a result of its partial oxidation/degradation during its polymerization and/or further processing.

Compared to the untreated PE, all of the modified samples showed a marked shift in IEP toward a higher pH, namely, higher than pH 3.2; this indicated that the surface was enriched with new basic functionalities. After chitosan coating, the function $ZP = f(\text{pH})$ showed a reversal of charge toward positive values, and later on, typical amphoteric characteristics and a shifting of the IEP toward higher pH regions were observed. At basic pH values, the negative streaming potential was due to deprotonation of the chitosan hydroxyl groups. The protonation of the chitosan amino groups (NH₃⁺) in the acidic region changed the sign of the streaming potential to a positive streaming potential at the IEP (pH ≈ 6.5). The higher amount of amino groups on the corona-treated and chitosan-coated samples explained the higher positive and negative values of ZP in the plateau of these samples. This was expected because chitosan coatings reduced the acidity of the PE film's surface.

The use of chitosan coatings with titratable end groups would be expected to produce changes in the ZP corresponding to the pK_a values of the respective end groups.³⁷ When the PE film was covered with chitosan, the IEP approached the pK value of chitosan; this was indicative of a proper surface coating. It is well known (and was demonstrated previously) that the amino

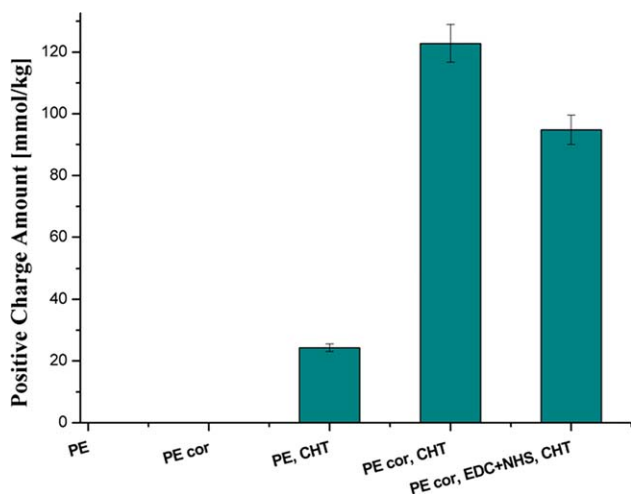


Figure 4. Amount of protonated amino groups on untreated, corona-treated, and chitosan-coated PE films determined by potentiometric titration. [Color figure can be viewed in the online issue, which is available at wileyonlinelibrary.com.]

groups in chitosan have a pK_a value of about 6.5.^{38,39} Therefore, it can be deduced from the graph presented in Figure 5 that a better coating of the PE surface was achieved when the substrate was corona-treated and further activated with a coupling agent solution, an assertion suggested by the fact that the IEPs for the PE_{cor}/CHT and PE_{cor}/EDC + NHS/CHT samples were closer to the pK_a value of chitosan.

Antimicrobial Tests. The modified/functionalized PE films were tested against two Gram-negative bacteria, *S. enteritidis* and *E. coli*, and one Gram-positive bacterium, *L. monocytogenes* (Figure 6 and Table V).

The antibacterial activity of the chitosan-modified PE films against all of the bacteria was evident; however, the influence of concentration was much more important in the case of *L. monocytogenes* (a conclusion drawn according to a study⁴⁰ of the influence of 1, 3, and 5 wt % concentrations of chitosan on the bacterial inhibitory action). This behavior could be explained by the fact that chitosan and/or its derivatives have been proven to be more effective against Gram-negative bacteria than against Gram-positive bacteria.⁴¹

The data presented in Table V reveal that the antibacterial activity of the grafted chitosan layer against all tested bacteria was similar for all of the chitosan-coated samples.

Figure 6 microscopically illustrates the way in which the bacterial colonies grown both in the absence (ATCC) and in the presence of the chitosan-coated PE films were inhibited.

According to the existing literature data, numerous factors affect chitosan's antibacterial effectiveness; these include microbial factors related to microorganism species and cell age; intrinsic factors of chitosan, including its positive charge density, molecular weight, concentration, hydrophilic/hydrophobic characteristics, and chelating capacity; its physical state, namely, the water-soluble and solid-state of chitosan; and environmental factors involving ionic strength in the medium, pH, temperature, and

reaction time.⁴² Therefore, the protonation and number of amino groups existing on the chitosan backbone, which are important in electrostatic interactions, play an important role in enhancing the antibacterial activity.

As shown in Table V, chitosan grafting did not affect its bactericidal efficiency, with the value for the PE_{cor}/EDC + NHS/CHT sample being similar to that of the PE_{cor}/CHT one. Even when some of chitosan's primary amino groups were involved in the coupling reaction, becoming less available for interacting with the bacterium cell wall, the remaining free amino groups were sufficient for inhibiting bacterial growth.

Desorption of Chitosan from the PE Surface

ATR-FTIR Spectroscopy Study of Chitosan Desorption. The chitosan-coated PE films, which were subjected to a desorption study at two different pH values, were taken from the desorption bath after 48 h and dried at 50°C *in vacuo*, after which their ATR-FTIR spectra were recorded. The IR spectra of the chitosan-coated PE films (corona-treated and activated with an EDC + NHS solution), as plotted in Figure 7, qualitatively revealed the presence of chitosan on the polymer surface, even after a 48-h desorption period.

After the desorption phase in a pH solution, both forms of amino group (NH_2 and NH_3^+) were likely to be present in the chitosan-coated samples, and we took into account the pK_a of the chitosan amine groups (ca. 6.5).⁴³ The protonation of chitosan amine functionalities was much more obvious for the PE_{cor}/CHT sample at pH 6.5 (Figure 7, spectrum 3); this was suggested by the presence of two peaks, both attributed to the NH_3^+ group, namely, the antisymmetrical deformation (δ_{as}) at 1633 cm^{-1} (a peak shoulder) and the symmetrical deformation

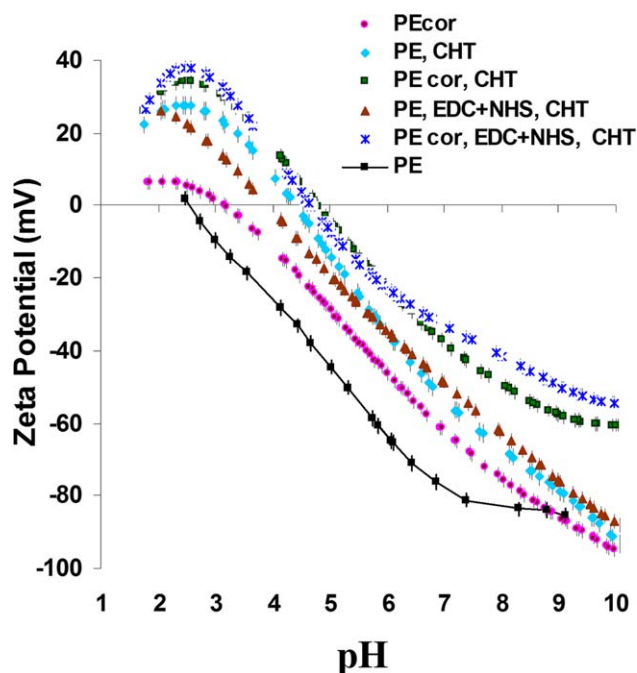


Figure 5. ZP versus pH (in aqueous solution of inorganic electrolyte, 1 mM KCl). [Color figure can be viewed in the online issue, which is available at wileyonlinelibrary.com.]

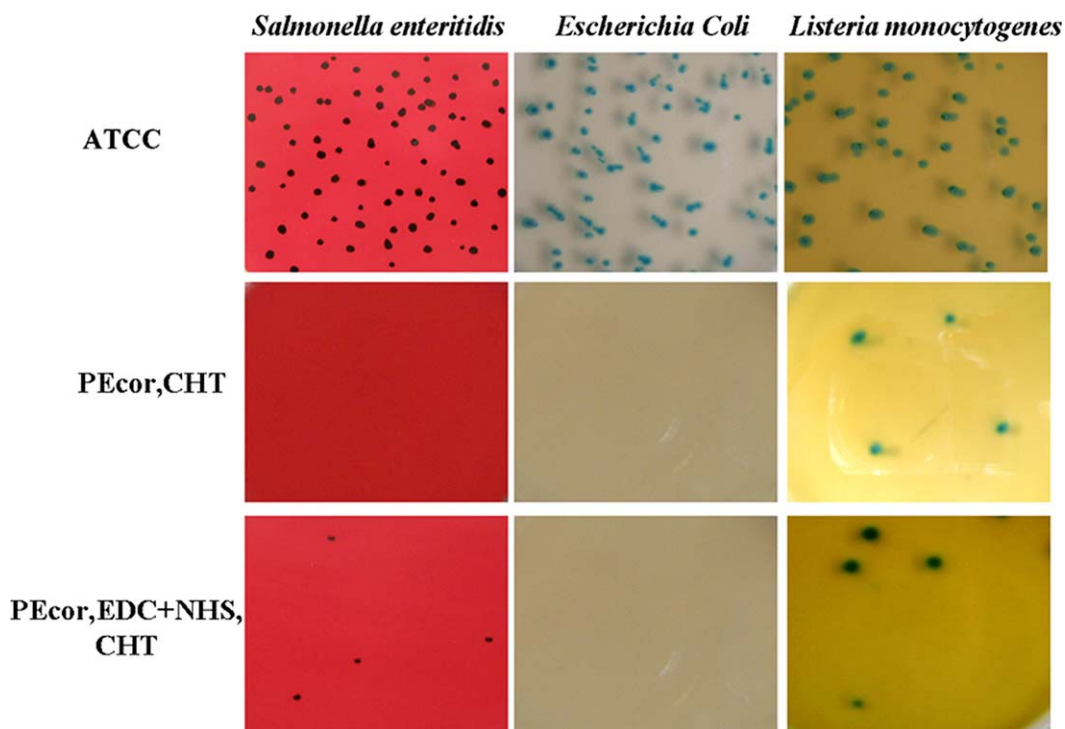


Figure 6. Microscopic aspects of the bacterial colonies grown in the absence (ATCC) and presence of the PE films coated with chitosan. [Color figure can be viewed in the online issue, which is available at wileyonlinelibrary.com.]

(δ_s) at 1575 cm^{-1} .⁴⁴ The initial amide I and II bands were possibly overlapped by these vibrations. On the other hand, the chitosan-coated PE sample, which was activated after corona treatment with a coupling agent solution, was less protonated after it was subjected to desorption, a phenomenon that could be explained by the lower number of free amino groups, which can be protonated easily and converted into amide groups [Figure 7 (spectrum 5); the peaks from 1651 and 1588 cm^{-1} assigned to amide I and amide II, respectively].

Gravimetric studies showed that for the PE_{cor}/CHT sample, the weight loss was larger than for the PE_{cor}/EDC + NHS/CHT one. For example, after it was with a pH 6.5 aqueous solution, the PE_{cor}/CHT sample had a weight loss of 50%, and the PE_{cor}/EDC + NHS/CHT sample had a weight loss of only 10% (for the corona-untreated sample, the weight loss was 100%). We, therefore, concluded that the chitosan layer deposited after the carbodiimide chemistry coupling reaction was much stable under various pH conditions than the other types of deposited layers.

Potentiometric Titration Results after the Desorption Step.

The amount of chitosan remaining on the surface was quantitatively determined by potentiometric titration. The PE films coated with chitosan were analyzed by potentiometric titration before and after desorption in different pH baths.

No significant difference was noticed between the protonated amino group amount found on the surfaces obtained by distinct immobilization strategies of chitosan, namely, by the physical adsorption (when the PE was corona-discharge-treated and then immersed in a chitosan solution) and grafting (PE was corona-discharge-treated and further chitosan was immobilized with coupling agents) methods. The main difference between these two methodologies refers to the stability of the obtained chitosan layer on the PE surface. In the case of grafting, a thin chitosan layer was irreversibly immobilized on the surface. Figure 8(a,b) provides two examples of potentiometric titration determination of the protonated amino group (positive charge) amount as a function of the desorption time.

A certain chitosan amount desorbed faster in solution, and equilibrium was reached in less than 24 h.

Table V. Antibacterial Activity of the Chitosan-Coated PE Surfaces

Sample composition	<i>S. enteritidis</i> inhibition: ATCC 25922, 48 h (%)	<i>E. coli</i> inhibition: ATCC 25922, 48 h (%)	<i>L. monocytogenes</i> inhibition: ATCC 25922, 48 h (%)
PE	39	14	25
PE _{cor} /CHT	100.0	100.00	92.59
PE _{cor} /EDC + NHS/CHT	92.77	100.00	95.83

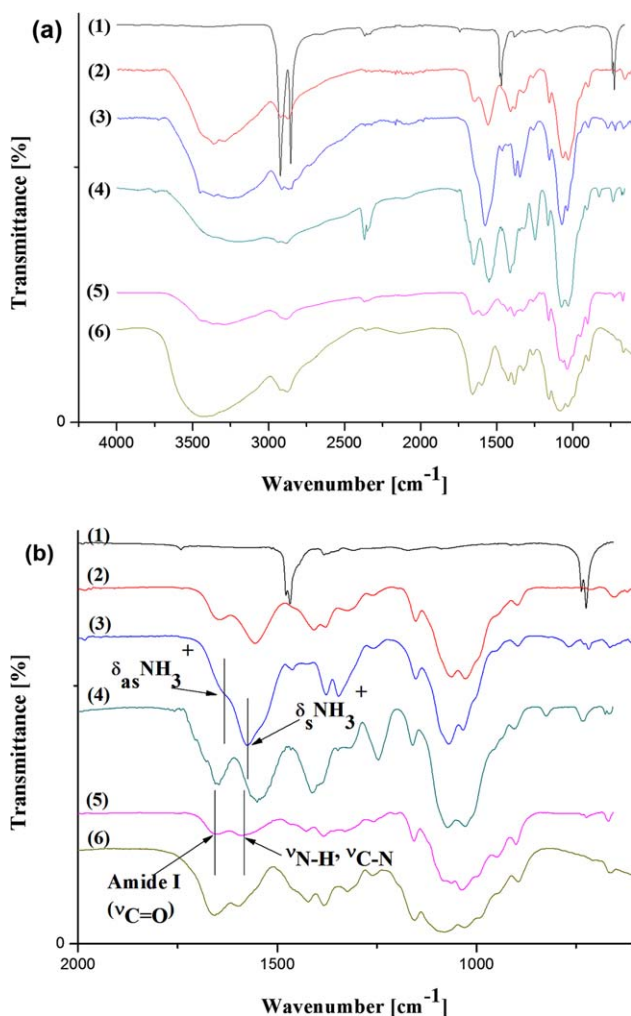


Figure 7. ATR-FTIR spectra of the chitosan-coated PE surfaces: (a) 4250–610 and (b) 2000–610 cm^{-1} . (1) PE; (2) PE_{cor}/CHT; (3) PE_{cor}/CHT, pH 6.5, 2880 min; (4) PE_{cor}/EDC + NHS/CHT; (5) PE_{cor}/EDC + NHS/CHT, pH 6.5, 2880 min; and (6) CHT. [Color figure can be viewed in the online issue, which is available at wileyonlinelibrary.com.]

After a 48 h of desorption, the surface charge amount calculated from the charge isotherms (Figure 9) was lower for PE_{cor}/CHT at pH 6.5 than for PE_{cor}/EDC + NHS sample at pH 6.5; this was due to the mass loss, which was much more significant for the first sample.

Chitosan-Desorption Study by Polyelectrolyte Titration.

Another method used for amino group determination on the PE films surface was an indirect one based on a photometric version of the polyelectrolyte titration of a chitosan-containing solution from the desorption bath.

Figure 10 illustrates the chitosan-desorption kinetic curves for corona-treated and chitosan-coated PE samples. For the corona-untreated PE film immersed in a chitosan solution, the polyelectrolyte titration is not shown, as no curve was obtained. The chitosan amount on the surface was undetectable by this method.

The main characteristic of all of the samples was that at pH 6.5, chitosan desorption was slower than in the desorption bath at

pH 3.5. This behavior could be explained by the fact that at acidic pH (3.5), all primary amino groups of chitosan were protonated (NH_3^+) and shifted more easily into solution.

A comparison between the PE_{cor} film coated with CHT and the chitosan-grafted sample (PE_{cor}/EDC + NHS/CHT) showed that in the mentioned sample, the chitosan amount desorbed from the surface was larger and that the process was oscillating at pH 6.5. In this case, chitosan desorption was quasi-reversible; this was possibly due to the unstable characteristics of the deposited chitosan layer on the surface. For instance, the chitosan amount determined at equilibrium in the desorption bath (pH 3.6) for PE_{cor}/CHT was three times higher than for PE_{cor}/EDC + NHS/CHT. In this way, the importance of the use of coupling agents for obtaining a stable layer of chitosan on top of the PE_{cor} film was once again highlighted.

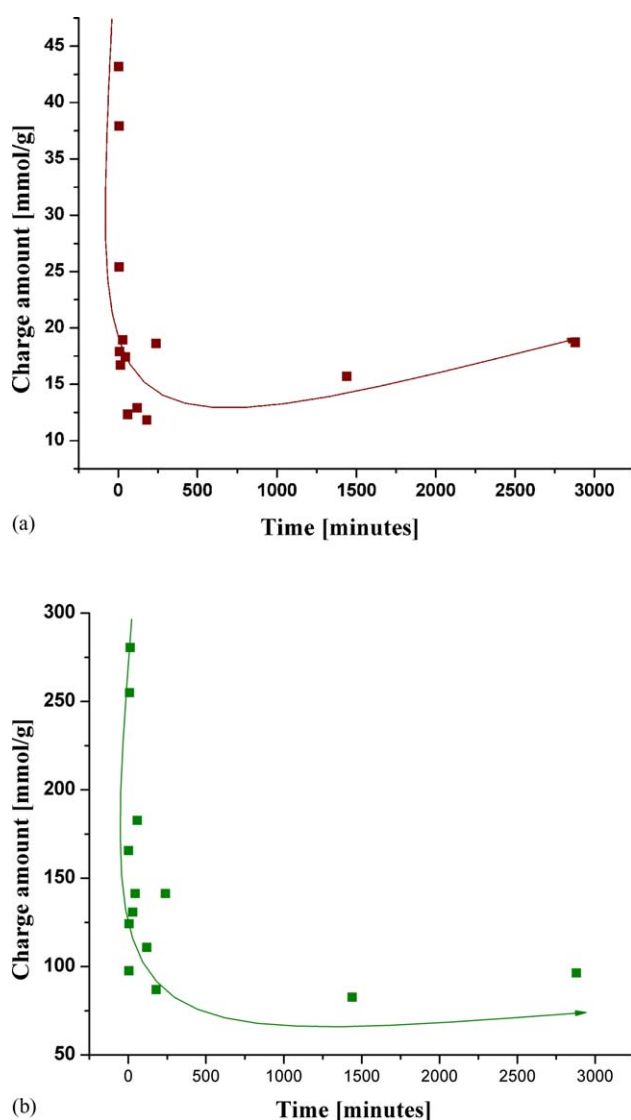


Figure 8. Kinetic desorption curves obtained by potentiometric titration for (a) PE_{cor}/EDC + NHS/CHT, pH 3.6, and (b) PE_{cor}/CHT, pH 3.6. [Color figure can be viewed in the online issue, which is available at wileyonlinelibrary.com.]

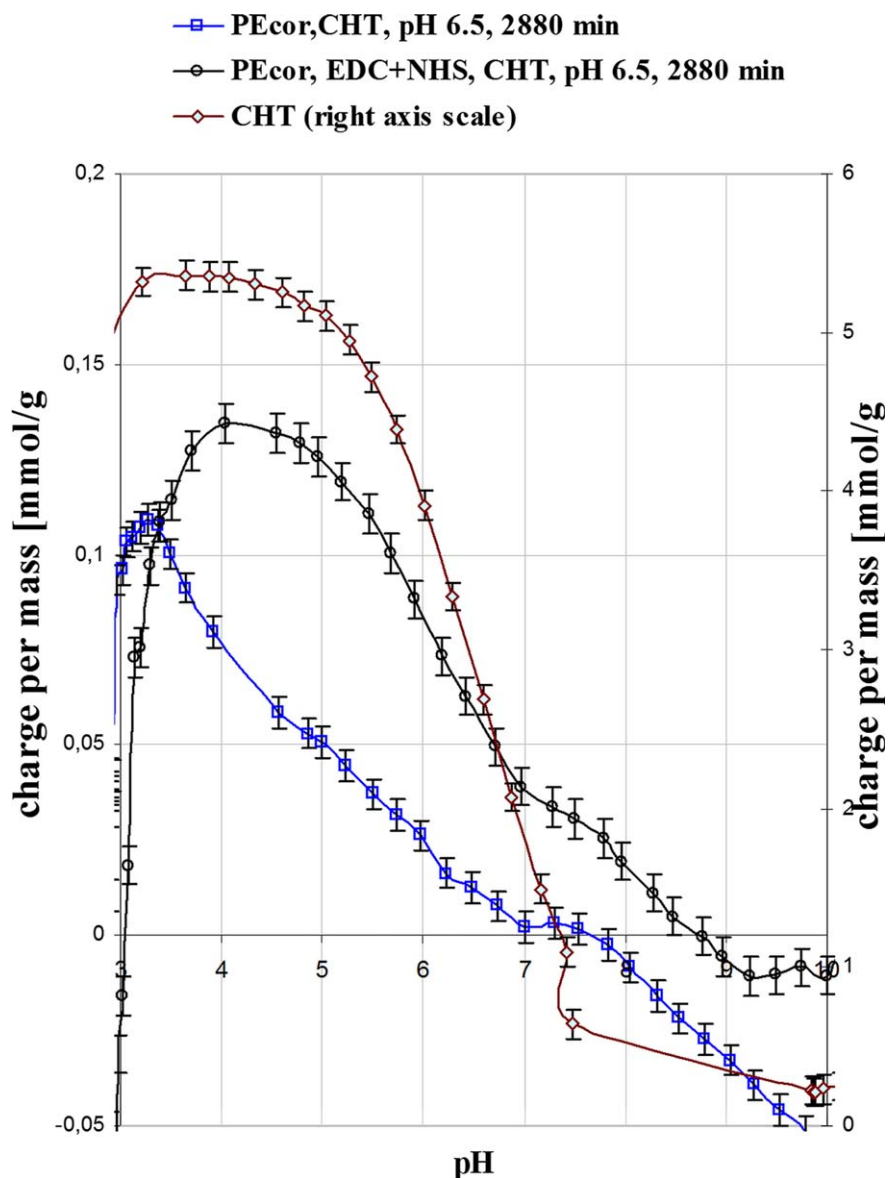


Figure 9. Potentiometric titration curves for PE_{cor}/CHT, pH 6.5, 2880 min, and PE_{cor}/EDC + NHS/CHT, pH 6.5, 2880 min, and titration curve for chitosan (CHT). [Color figure can be viewed in the online issue, which is available at wileyonlinelibrary.com.]

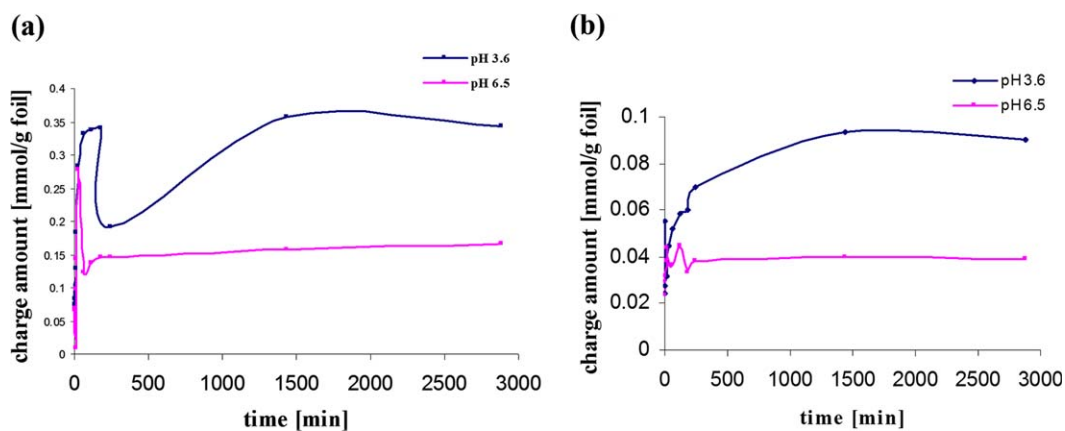


Figure 10. Kinetic desorption curves of chitosan at two different pHs (3.6 and 6.5): (a) PE_{cor}/CHT and (b) PE_{cor}/EDC + NHS/CHT. [Color figure can be viewed in the online issue, which is available at wileyonlinelibrary.com.]

The potentiometric titration results showed a good correlation with the polyelectrolyte titration data. Both methods showed that for the corona-treated samples, a certain amount of chitosan desorbed faster in solution and reached equilibrium in less than 24 h (Figure 8). The difference between these two methods was that the potentiometric titration determined the protonated amino group (charge) amount on the surface, whereas the polyelectrolyte titration determined the protonated amino groups desorbed from the PE surface. In the last case, the analyzed sample was the solution obtained from the desorption baths. ATR–FTIR spectroscopy qualitatively supported the conclusion drawn from the titration techniques, that only a certain amount of chitosan desorbed from the PE_{cor} surface. This was evidenced by a decrease in chitosan's characteristic peak intensities after desorption, even when some amount of chitosan still remained on the surface, as mentioned previously.

CONCLUSIONS

The corona-discharge treatment of PE induced physicochemical surface modifications, mainly by the implantation of oxygen-containing groups on the surface, because of the interactions between the polymer surface and the reactive species present in the corona system. This step created a favorable surface environment for chitosan adsorption/grafting.

Two complementary methodologies were developed for the antibacterial chitosan immobilization on PE films, namely, physical adsorption and grafting.

The formation of new oxygen-containing functionalities after corona treatment and amine and amide groups after chitosan coating/grafting were detected and analyzed by ATR–FTIR and XPS spectroscopy. We established that chitosan was attached only to the PE_{cor} surface. A corona-discharge treatment coupled with chemical activation with EDC and NHS led to covalent bonding of the chitosan on the PE surface, mainly by the formation of amide groups and other types of linkages, and a stable surface layer of chitosan thus resulted.

Potentiometric and polyelectrolyte titrations showed that a certain amount of chitosan desorbed faster from the surface until equilibrium was reached and also that the covalently attached chitosan layer was more stable than the physically adsorbed one.

The chitosan immobilized on the PE surface exhibited the expected antibacterial activity when tested against three bacteria, two Gram-negative ones, *S. enteritidis* and *E. coli*, and one Gram-positive bacterium, *L. monocytogenes*.

The corona-discharge treatment of PE, a known industrially applied technology, followed by coating with chitosan, proved to be very useful for the appropriate modification of its surface properties. Furthermore, a chemical coupling system is needed to obtain a stable surface chitosan layer that can lead to an antibacterial PE surface useful for food packaging or medical devices that prevent bacterial attachment and achieve anti-infection properties. Furthermore, the covalently attached chitosan layer prevented the undesirable migration of bioactive components in the surrounding media.

ACKNOWLEDGMENTS

The authors acknowledge the financial support of the European Cooperation in Science and Technology action FA0904 (Eco-Sustainable Food Packaging Based on Polymer Nanomaterials), of Bilateral cooperation Romania-Slovenia: Functionalization of Synthetic Polymers for Development of new Antimicrobial Packaging Department, and the Food Safety Department, Veterinary and Food Safety Laboratory, Iasi, Romania, offered by Biochem Gina Pricope for antibacterial tests.

REFERENCES

- Vasilev, K.; Cook, J.; Griesser, H. *J. Expert Rev. Med. Devices* **2009**, *6*, 553.
- Wang, J.; Huang, N.; Pan, C. J.; Kwok, S. C. H.; Yang, P.; Leng, Y. X.; Chen, J. Y.; Sun, H.; Wan, G. J.; Liu, Z. Y.; Chu, P. K. *Surf. Coat. Technol.* **2004**, *186*, 299.
- Shintani, H. *Trends Biomater. Artif. Organs* **2004**, *18*, 1.
- Nur Dirim, S.; Özlem Özden, H.; Bayındırlı, A.; Esin, A. *J. Food Eng.* **2004**, *63*, 9.
- Tokura, S.; Ueno, K.; Miyazaki, S.; Nishi, N. *Macromol. Symp.* **1997**, *120*, 1.
- Tsai, G. J.; Su, W. H.; Chen, H. C.; Pan, C. L. *Fisheries Sci.* **2002**, *68*, 170.
- Begin, A.; Van Calsteren, M. *Int. J. Biol. Macromol.* **1999**, *26*, 63.
- Bourtoom, T. *Int. Food Res. J.* **2008**, *15*, 237.
- Park, S. I.; Marsh, K. S.; Dawson, P. L.; Acton, J. C.; Han, I. IFT Annual Meeting Book of Abstracts; Institute of Food Technologists: Anaheim, CA, **2002**; Paper No. 100B-23, p. 250.
- Darie, R. N.; Cheaburu, C. N.; Pricope, G. N.; Constantinescu, D.; Vasile, C. *Rom. Pat. Appl. OSIM A/00807/11.08* (**2011**).
- Eriksson, J. C.; Golander, C. G.; Baszkin, A.; Terminassian-saraga, L. *J. Colloid Interface Sci.* **1984**, *100*, 381.
- Larsson, R.; Eriksson, J. C.; Olsson, P. *Thromb. Res.* **1979**, *14*, 941.
- Lin, C. H.; Lin, J. C.; Chen, C. Y.; Cheng, C. Y.; Lin, X. Z.; Wu, J. J. *J. Appl. Polym. Sci.* **2005**, *97*, 893.
- Shi, J. L.; Kang, E. T.; Neoh, K. G.; Tan, K. L.; Liaw, D. *J. Eur. Polym. J.* **1998**, *34*, 1429.
- Robertson, G. L. *Food Packaging: Principles and Practice*; Marcel Dekker: New York, **1993**.
- Shin, G. H.; Lee, Y. H.; Lee, J. S.; Kim, Y. S.; Choi, W. S.; Park, H. J. *J. Agric. Food Chem.* **2002**, *50*, 4608.
- Theapsak, S.; Watthanaphanit, A.; Rujiravanit, R. *Am. Chem. Soc. Appl. Mater. Interfaces* **2012**, *4*, 2474.
- NHS and Sulfo-NHS. Thermo Scientific. <http://www.pierce-net.com/browse.cfm?fldID=02040114> (accessed March 2013).
- Zhao, C.; Sun, Y. L.; Kirk, R. L.; Thoreson, A. R.; Jay, G. D.; Moran, S. L.; An, K. N.; Amadio, P. C. *J. Bone Joint Surg. Am.* **2010**, *92*, 1453.
- Anderson, G. L.; McIntosh, M.; Wu, L.; Barnett, M.; Goodman, G.; Thorpe, J. D.; Bergan, L.; Thornquist, M. D.; Scholler, N.; Kim, N.; O'Briant, K.; Drescher, C.; Urban, N. *J. Natl. Cancer Inst.* **2010**, *102*, 26.

21. Frasc, L.; Laine, J.; Stenius, P.; Stana-Kleinschek, K.; Ribitsch, V.; Doleček, V. *J. Appl. Polym. Sci.* **2004**, *92*, 3186.
22. Cheng, Y.; Luo, X.; Betz, J.; Buckhout-White, S.; Bekdash, O.; Payne, G. F.; Bentley, W. E.; Rubloff, G. W. *Soft Matter* **2010** [Supplementary Material (ESI)].
23. Elimelech, M.; Chen, W. H.; Waypa, J. *J. Desalination* **1994**, *95*, 269.
24. Peeters, J. M. M.; Mulder, M. H. V.; Strathmann, H. *Colloids Surf. A* **1999**, *150*, 247.
25. Fievet, P.; Sbai, M.; Szymczyk, A.; Vidonne, A. *J. Membr. Sci.* **2003**, *226*, 227.
26. Bismarck, A.; Kumru, M. E.; Springer, J. *J. Colloid Interface Sci.* **1999**, *217*, 377.
27. Szymczyk, A.; Pierre, A.; Reggiani, J. C.; Pagetti, J. *J. Membr. Sci.* **1997**, *134*, 59.
28. Saraswathy, G.; Pal, S.; Rose, C.; Sastry, T. P. *Bull. Mater. Sci.* **2001**, *24*, 415.
29. Balaban, A. T.; Baciu, M.; Pogany, I. I. Applications of the Physical Methods in Organic Chemistry; Scientific and Pedagogical-House: Bucharest, **1983**; p 18.
30. Chen, Z.; Mo, X.; He, C.; Wang, H. *Carbohydr. Polymer* **2008**, *72*, 410.
31. Briggs, D.; Seah, M. P. Practical Surface Analysis by Auger and X-ray Photoelectron Spectroscopy; Wiley: Chichester, United Kingdom, **1988**.
32. Takahashi, K.; Shizume, R.; Uchida, K.; Yajima, H. *J. Bioreol.* **2009**, *23*, 64.
33. Yap, W. F.; Yunus, W. M. M.; Talib, Z. A.; Yusof, N. A. *Int. J. Phys. Sci.* **2011**, *6*, 2744.
34. Liu, Y.; Gaskell, K. J.; Cheng, Z.; Yu, L.; Payne, G. F. *Langmuir* **2008**, *24*, 7223.
35. Beneš, P.; Paulenová, M. *Colloid Polym. Sci.* **1973**, *251*, 766.
36. Temmel, S.; Kern, W.; Luxbacher, T. *Progr. Colloid. Polym. Sci.* **2006**, *132*, 54.
37. Dougherty, G. M.; Rose, K. A.; Tok, J. B. H.; Pannu, S. S.; Chuang, F. Y. S.; Sha, M. Y.; Chakarova, G.; Penn, S. G. The Zeta Potential of Surface-Functionalized Metallic Nanorod Particles in Aqueous Solution; UCRL-JRNL-230853; <https://e-reports-ext.llnl.gov/pdf/347379.pdf>.
38. Park, J. W.; Choi, K. H. *Bull. Kor. Chem. Soc.* **1983**, *4*, 68.
39. Zentz, F.; Bédouet, L.; Almeida, M. J.; Milet, C.; Lopez, E.; Giraud, M. *Mar. Biotechnol.* **2001**, *3*, 36.
40. Munteanu, B. S.; Păslaru, E.; Frasc-Zemljic, L.; A. Sdrobis, Pricope, G.; Vasile, C. *Cell. Chem. Technol.*, accepted.
41. Chen, Y. M.; Chung, Y. C.; Wang, L. W.; Chen, K. T.; Li, S. Y. *J. Environ. Sci. Health A* **2002**, *37*, 1379.
42. Kong, M.; Chen, X. G.; Xing, K.; Park, H. *J. Int. J. Food Microbiol.* **2010**, *144*, 51.
43. Domard, A. In Advances in Chitin Science; Domard, A., Roberts, G., Vårum, K., Eds.; Jacques André: Lyon, **1997**; Vol. 2, p 410.
44. Pearson, F. G.; Marchessault, R. H.; Liang, C. Y. *J. Polym. Sci.* **1960**, *43*, 101.